Available online at www.sciencedirect.com
ScienceDirect
Microporous and Mesoporous Materials 114 (2008) 281–292
MICROPOROUS AND MESOPOROUS MATERIALS
www.elsevier.com/locate/micromeso

Spectroscopic and catalytic characterization of Co-exchanged mordenites subject to CO/O_2 redox treatments

L. Gutierrez [a], E. Miró [a,*], S. Irusta [b]

[a] *Instituto de Investigaciones en Catálisis y Petroquímica (FIQ, UNL-CONICET), Santiago del Estero, 2829-3000 Santa Fe, Argentina*
[b] *Instituto de Nanociencia de Aragón, Universidad de Zaragoza, Pedro Cerbuna 12-50009, Zaragoza-España, Spain*

Received 18 May 2007; received in revised form 2 January 2008; accepted 8 January 2008
Available online 15 January 2008

Abstract

Co-mordenites were prepared by ion exchange and wet impregnation over Na-mordenite and H-mordenite. The prepared solids were calcined and aliquots of these samples were subject to redox treatments first with CO for 2 h at 773 K and then kept 2 h at the same temperature in flowing O_2. A thorough characterization of the solids was carried out by TPR, XPS, CO volumetric adsorption, and FTIR with CO, NO and pyridine adsorption as probe molecules. After the redox treatment, Na based samples showed an important increase in the CO adsorption. TPR and XPS results indicated reduction of the oxides present in the calcined samples and the migration of exchanged cobalt from hidden to more exposed sites was demonstrated by FTIR. The acid catalysts did not change their CO capacity of adsorption; exchanged cobalt ions were mainly in β-type sites and remained in this position after treatment. After the redox treatments, the activity for the selective reduction of NO_x with methane suffered a decrease on both types of mordenites, probably caused by the strong adsorption of NO and the reduction of β-type Co^{2+} to metallic cobalt that would diminish the active sites concentration and also block the channels, thus preventing the access of the reactants.

Keywords: Co-mordenite; Redox treatment; CO adsorption; NO adsorption; Cobalt species on the SCR

1. Introduction

Since Li and Armor [1] reported that CH_4 is an effective reducing agent for NO_x SCR when Co-ZSM-5 or CoFerrierite catalysts are used, Co-exchanged zeolites have been extensively studied both in their kinetic [2–4] and characterization aspects [5–7]. Upon exchange procedure, different cobalt species can be formed in a zeolitic framework, i.e. Co^{2+} at exchange sites, CoO_x species inside zeolite pores, and well-developed Co oxides on the external surface of zeolite crystals. It has been demonstrated that Co^{2+} at exchange sites is the active species for the NO_x SCR with methane and that the formation of CoO_x and Co_3O_4 species causes catalyst deactivation [3].

The migration of exchanged ions inside zeolitic frameworks has been observed for different systems and conditions [8,9]. Miró and Petunchi [10] reported that redox treatments on a Co-mordenite sample with CO/O_2 at 723 K strongly increased CO chemisorption and catalytic activity for CO oxidation. The reaction rate for the $CO + O_2$ reaction increased by three orders of magnitude and the heat of adsorption increased from 39.7 to 48.1 kJ-mol^{-1} after the redox treatment. These results were analyzed in terms of the mobility of cations from hidden to accessible sites in the mordenite framework, but at that time that possibility could not be demonstrated. Later, Fierro et al. [11] reported a thorough study of the redox chemistry of Co-ZSM-5 zeolite, using CO/O_2 and H_2/O_2 as redox couples. However, they did not analyze the possibility of ion migration from one exchange site to another during the redox treatment. Since they used fully exchanged samples, most probably the mobility phenomenon could not be

* Corresponding author.
E-mail address: emiro@fiq.unl.edu.ar (E. Miró).

1387-1811/$ - see front matter © 2008 Elsevier Inc. All rights reserved.
doi:10.1016/j.micromeso.2008.01.014

observed. They found a $O/Co \approx 0.5$ ratio during CO/O_2 redox cycles and, since Co^{1+} is not a stable ion, they explained this behavior by the chemistry involved in the preparation. The principal ion present in their exchange solution (cobalt acetate, pH 4.5) was $[CoOH]^+$. Thus, during the drying step, reaction $2\ Co^{2+}OH^- \rightarrow Co^{2+}—O—Co^{2+} + H_2O$ was likely to occur and one extra lattice oxygen (ELO) would be introduced. Carbon monoxide can easily remove this ELO trough reaction $Co^{2+}—O—Co^{2+} + CO \rightarrow Co^{2+} + Co^0 + CO_2$.

The formation of metallic cobalt upon the CO treatment at 723 K can catalyze the Boudouard reaction ($2\ CO \rightarrow C + CO_2$). This phenomenon was reported by Miró and Petunchi [10]. After the oxygen treatment, they observed an $O/Co \approx 0.3$ ratio during CO/O_2 redox cycles for Co-mordenite, which is lower than that observed by Fierro et al. [11] for Co-ZSM-5 and, as stated above, the CO adsorption capacity and CO oxidation rate significantly increased. The structure of exchanged mordenite allowed the possibility of Co migration from the side-pockets to the main channels [12], thus explaining the behavior observed. CO could be freely adsorbed on Co located in the main channels but this was difficult when the cobalt ions were located in the side-pockets. The absence of side-pocket sorption was reported by Sefcik et al. [13] for CO and CO_2 on H^+, K^+, Cs^+ and NH_4^+ exchanged mordenite.

The objective of the present work is to characterize the behavior of different prepared Co-mordenites upon redox cycles with CO/O_2. The catalysts are characterized by XPS, LRS, XRD, FTIR and CO chemisorption. The acidic properties of prepared solids are investigated by FTIR using pyridine as probe molecule. The relevance of different redox states of cobalt on the SCR of NO_x with CH_4 as test reaction is also addressed.

2. Experimental

2.1. Catalyst preparation

The catalysts were prepared by ion exchange and wet impregnation starting from Na-mordenite (Na-MOR) manufactured by Zeolyst International Na-MOR-Z (Product ID: CBV 10A; Lot. N° 1822-50, Si/Al = 6.5) and by Linde Na-MOR-L (LZM5 lot 8350-5, Si/Al = 5). The ion exchanged forms, H-mordenite (H-MOR) and Co,H-mordenite were prepared following the procedure described by Gutierrez et al. [14]. Briefly, H-MOR was obtained using a solution of NH_4NO_3 keeping it on reflux for 24 h at 373 K. An aliquot of H-MOR was exchanged with a solution of $Co(CH_3COO)_2$. After the exchange, the solids were filtered, washed, and dried. The solids prepared were Co–Na–L (3.24 Co wt%), Co–H–L (2.62 Co wt%), Co–Na–Z (2.91 Co wt%) and Co–H–Z (2.91Co wt%).

In order to characterize Co oxide species supported on the mordenite framework, Co/H–Z and Co/Na–Z were prepared by the standard wet impregnation method, thus favoring the formation of oxide species. The impregnation was carried out using the exact amount of desired cobalt on a $Co(CH_3COO)_2$ solution (zeolite/solution ratio = 8 g/L), the cobalt content being 1.42 and 1.38 wt%, respectively.

All samples were treated following two different procedures: (A) heating the samples up to 773 K in N_2 flow and keeping at this temperature for 8 h; then, they were treated with O_2 at the same temperature for 2 h. We call these samples "calcined". An aliquot of these calcined samples was treated as follows: (B) heating up 5 °C/min in flowing nitrogen to 773 K, then in a stream of 25% CO for 2 h; after switching back to N_2, the samples were kept at the same temperature in flowing O_2 for 2 h. We define these samples "CO treated". Table 1 shows the Co content of the prepared samples.

2.2. Temperature-programmed reduction (H_2-TPR)

These experiments were carried out with 0.05–0.10 g of either the fresh or treated catalyst using an Okhura TP-2002S instrument equipped with a TCD detector. Prior to the TPR measurements, the solids were pretreated in Argon heating up to 773 K at 2 K min^{-1}. The reducing gas was 5% H_2/Ar mixture. The flow rate was 30 $cm^3\ min^{-1}$. The temperature was ramped up at a rate of 10 K min^{-1} to 1093-1173 K.

2.3. CO adsorption

Volumetric CO adsorption experiments were run at 298 K in a conventional B.E.T. system capable of obtaining a vacuum of 1.3×10^{-4} Torr. It was connected to a gas recirculation loop to allow *in situ* pretreatment of the solids. The reactor was loaded with 0.3 g of sample.

2.4. FTIR study

2.4.1. CO adsorption

The IR spectra were obtained using a Shimadzu FTIR 8101M spectrometer with a spectral resolution of 4 cm^{-1}. The samples were prepared by compressing the solids at 4×10^8 Pa in order to obtain a self-supporting wafer (0.05 g, 1 cm diameter). They were mounted on a transportable infrared cell with CaF_2 windows and external oven. The pretreatment was performed in a high vacuum system. The sample was first outgassed at 723 K for 12 h in a dynamic vacuum of 7×10^{-4} Pa. It was then cooled to room temperature and CO was introduced into the cell.

2.4.2. NO adsorption

These experiments were carried out in a Fourier-transform infrared spectrometer (FTIR), Thermo Matson Genesis II. Finely powdered catalyst samples were pressed (6.10^8 Pa, 5 min) into self-supporting wafers. Each wafer was inserted into a quartz sample holder with a furnace for the *in situ* activation of the sample. The sample holder was attached to the IR cell with F_2Ca windows. After the pretreatment program, it was allowed to cool to room

temperature and the spectrum of the activated sample was collected. The adsorption procedure involved contacting the activated wafer with NO at RT for 15 min and outgassing with He to remove the NO gas-phase. Then, the temperature was increased in steps (373, 393, 423, 473, 523, 575, 623 and 673 K) and an FTIR spectrum at RT was collected after each step. The spectra of adsorbed NO species following each evacuation step were obtained by subtracting the spectrum of the activated wafer.

2.4.3. Pyridine adsorption

The species formed on the catalyst surface after pyridine adsorption were monitored by infrared spectroscopy using a Thermo Matson Genesis II spectrometer and a conventional glass infrared cell equipped with CaF_2 windows and a built-on furnace for the in situ activation of the sample. Finely powdered catalyst samples were pressed into self-supporting pellets with a "thickness" of 10–11 mg cm^{-2}. The sample was heated up to 673 K under continuous evacuation at a heating rate of 5 K min^{-1} and was pretreated at 673 K for 4 h. Then it was allowed to cool to room temperature and the spectrum of the activated sample was collected. 2 μL of pyridine was added to the chamber by a Hamilton syringe. Then the pyridine vapor was removed from the cell by evacuation at RT for 20 min. Additional evacuation was carried out at 723 K for 20 min. A new spectrum was measured at room temperature after each evacuation step by collecting 40 scans at a nominal resolution of 4 cm^{-1}. The adsorption spectra of adsorbed pyridine species following each evacuation step were obtained by subtracting the spectrum of the activated pellet. Finally, all the different spectra were normalized to a standard density of 10 mg cm^{-2}.

2.4.4. Surface analysis by XPS

The X-ray photoelectron analyses were performed with an Axis Ultra DLD (Kratos Tech.). The spectra were excited by the monochromatized AlKα source (1486.6 eV) run at 15 kV and 10 mA. For the individual peak regions, pass energy of 20 eV was used. Survey spectra were measured at 160 eV pass energy. Analyses of the peaks were performed with the software provided by Kratos, using a properly weighted sum of Lorentzian and Gaussian components curves after background subtraction according to Shirley and Sherwood. All binding energies were corrected for charging by assuming the binding energy of the C1s band to be 284.9 eV.

2.4.5. Catalytic test

The catalyst powders were tested in a continuous flow, fixed-bed, quartz micro reactor. All catalysts were tested after each pre-treatment (A and B). The typical composition of the reactant stream was the following: 1000 ppm CH_4, 1000 ppm NO and 2% O_2 in He (GHSV: 7500 h^{-1}). The composition of the reactor effluent was monitored for CH_4, CO, NO, N_2O and NO_2 by a Fourier-transform infrared spectrometer (FTIR), Thermo Matson Genesis II, equipped with a gas IR cell, having a 15 cm path length.

The CH_4 to CO_2 and the NO_x to N_2 conversions were defined as $C_{NOx} = (1 - [NO_x]/[NO_x]^o) \times 100$, and $C_{CH4} = (1-[CH_4]/[CH_4]^o) \times 100$. $[NO_x]^o$ and $[CH_4]^o$ stand for the NO and CH_4 concentration of the feed, respectively. N_2 was measured by nitrogen balance.

3. Results

3.1. TPR

The TPR results of the prepared samples are shown in Table 1 and Fig. 1. In all the reduction curves two zones can be distinguished: SI (373–923 K) corresponding to those kinds of cobalt species with high or moderate oxide characteristics (Co_3O_4 crystals, oxo-cations $[Co{-}O{-}Co]^{2+}$ and CoO_x stabilized inside the zeolite), and SII (923–1173 K) to Co^{2+} at exchange positions in the zeolite.

Co–Na–L: The profile of the calcined sample presents a broad reduction zone in the 373–923 K temperature range; it probably consists of two overlapping peaks due to the reduction of Co oxides and CoO_x species stabilized in the zeolitic matrix. The H_2 consumption (Table 1) indicates that cobalt is as Co^{2+} (H_2 total/Co = 1) and that 78% of it is at exchange position (SII). After the CO treatment the hydrogen consumption in the 373–923 K range diminishes, two small peaks at ca 573 K and 773 K are observed and the SII species increase up to 86%.

Co–H–L: the calcined sample presents only 9% of Co as SI species and after the CO treatment this peak shifts to slightly higher temperatures. There are no peaks up to 1173 K, suggesting that the Brønsted acidity of the zeolite leads cobalt to more stable positions [15].

Co–Na–Z: 9% of SI is present in the calcined sample and the reduction zone of SII species shows two overlapping peaks, suggesting that there are Co^{2+} at exchange positions

Table 1
Effect of the pretreatment on the reducibility of the prepared samples

Catalyst (μmol Co)[a]	Treatment	H_2/Co[b]		
		373–923 K	923–1173 K	Total
Co–Na–L	O_2	0.24	0.78	1.02
(54.91)	CO	0.07	0.86	1.0
Co–H–L	O_2	0.09	–	–
(44.41)	CO	0.06	–	–
Co–Na–Z	O_2	0.09	0.75	0.84
(49.32)	CO	0.04	0.77	0.81
Co–H–Z	O_2	0.10	0.68	0.78
(49.32)	CO	0.06	0.07	0.13
Co/Na–Z	O_2	0.71	0.48	1.19
(23.39)	CO	0.60	0.35	0.95
Co/H–Z	O_2	0.86	0.11	0.97
(24.07)	CO	0.53	–	–

[a] μmoles per 0.1 g sample.
[b] Molar ratio.

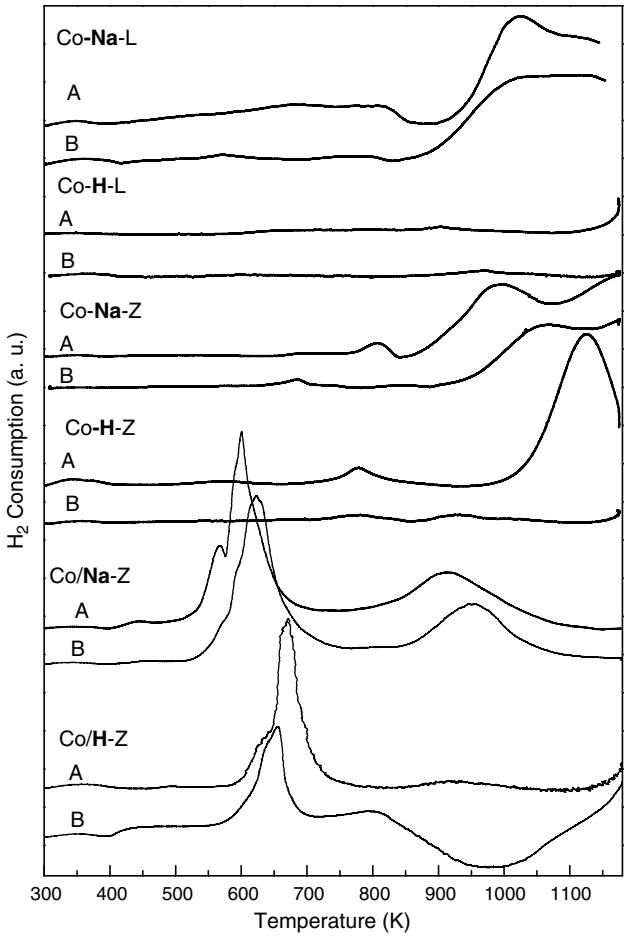

Fig. 1. TPR profiles of samples prepared by ion exchange and wet impregnation: (A) calcined O_2, (B) treated with CO.

in the 12-member ring channels, and in the mordenite side-pockets [16]. When the sample is treated with CO, the amount of SI species is lower than in the calcined solid and the maximum of the overlapping peak shifts to higher temperatures. This would indicate that Co species are less reducible after the CO treatment; another possibility is that part of the Co oxide was reduced to metallic cobalt by the treatment.

Co–H–Z: 10% of SI is observed in the calcined sample. Co SII species in the H-MOR matrix reduce at higher temperatures than in the Na-MOR solid. After the treatment with CO, the reduction takes place at temperatures higher than 1173 K while no SI species are observed.

Co/Na–Z: The H_2/Co ratio in the calcined sample suggests the presence of Co_3O_4 besides the Oxo-Co species (373–673 K range). The peak at 923 K corresponds to cobalt at exchange positions, which could have been formed during the impregnation and stabilized during the calcination. In this case, the presence of cobalt oxides leads to a Co/H_2 ratio higher than 1 because the stoichiometry of the cobalt oxide reduction is $H_2/Co_3O_4 = 1.33$. When the sample is treated with CO some differences can be observed: the higher temperature peak shifts to 953 K, the reduction temperature of SI species increase ca. 20 K and H_2/Co ratio is lower than 1. Even in impregnated samples there are changes in the reducibility of species as a consequence of the CO treatment.

Co/H–Z: In this particular sample a negative peak is observed at high temperature. This effect may be due to the presence of some carbonaceous species formed during the treatment with CO and they were not re-oxidized after the second stage of the pretreatment, i.e. calcinations. In Co/Na–Z sample this effect was not observed suggesting that the acidity of the zeolite matrix might contribute to the formation of such species. On the other hand, the hydrogen consumption in the 373–673 K range decreased almost 40% (Table 1).

The TPR results show that for all Co-exchanged zeolites, the presence of cobalt oxides decreases after the redox treatment. Sodium catalysts also show an increase in the exchanged cobalt, but nothing can be said about acid zeolites since the reduction temperatures are higher than the upper limit temperature of our TPR equipment, indicating that the exchanged Co ions are in less reducible sites than in Na catalysts. This could be probably explained by the fact that in the H-MOR-type zeolite the Co is stabilized in higher coordinated sites than in the Na-MOR starting solid. Kaucký et al. reported an exhaustive quantification of the relative concentration of Co ions on α, β and γ on CoNaKFer and CoHFer [15]. On the other hand, the TPR of impregnated solids also shows the presence of some exchanged cobalt cations and the redox treatment affects the reducibility of the species again. Nevertheless, the main TPR peaks in the impregnated samples correspond to oxide species.

3.2. CO adsorption

Fig. 2 shows the adsorption isotherms at 298 K for calcined and CO treated Co–Na (Co–Na–L, Co–Na–Z and Co/Na–Z). After the CO treatment, the CO adsorption capacity was increased in these solids; this is in agreement with the observations of Miró and Petunchi [10], who reported the increase in CO adsorption capacity of Co–Na-MOR (Si/Al = 5) after pre-treatment with CO and O_2 at high temperatures and explained it by the mobility of Co from sites in the side-pockets to sites in the main channel. On the other hand, the Co–H (Co–H–L, Co–H–Z and Co/H–Z) CO adsorption capacity was not modified by the CO treatment (Fig. 3). The counter cations would play an important role in the CO adsorption capacity of the Co mordenite after the redox treatment, while the Si/Al ratio of the zeolite matrix would play a less important role. From Figs. 2 and 3, it can also be noted that on calcined samples, while Co–H–Z adsorbs more CO than Co–Na–Z, Co–H–L and Co–H–Z adsorb similar amounts. This could be due to a combined effect of acidity and accessibility properties. Both Co–H–Z and Co–H–L have acid sites that can favour CO adsorption, but exchanged cobalt ions in Co–H–L are more stable than in Co–Na–L as shown in the TPR profiles.

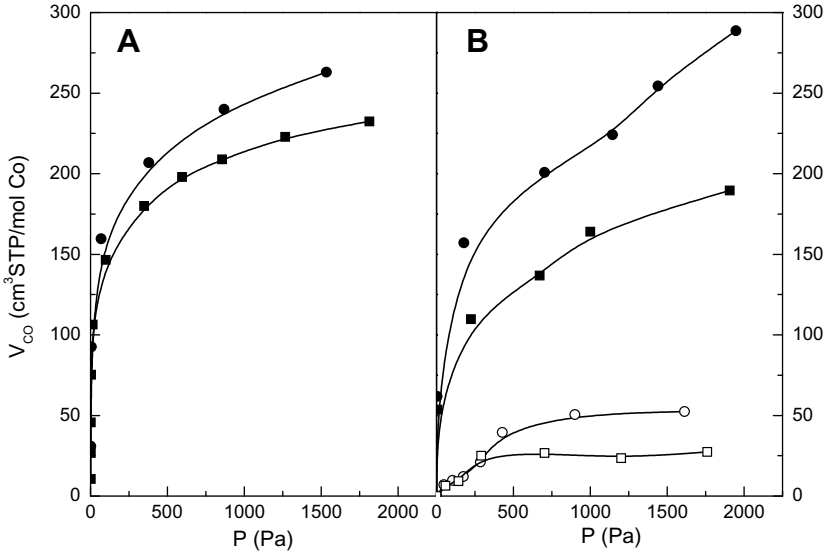

Fig. 2. CO adsorption isotherm at 298 K. (A): Co–Na–L, (B): Co–Na–Z and Co/Na–Z. ●, ○: CO treated, ■, □: calcined. Closed symbol: prepared by ionic exchange, open symbol: prepared by wet impregnation method.

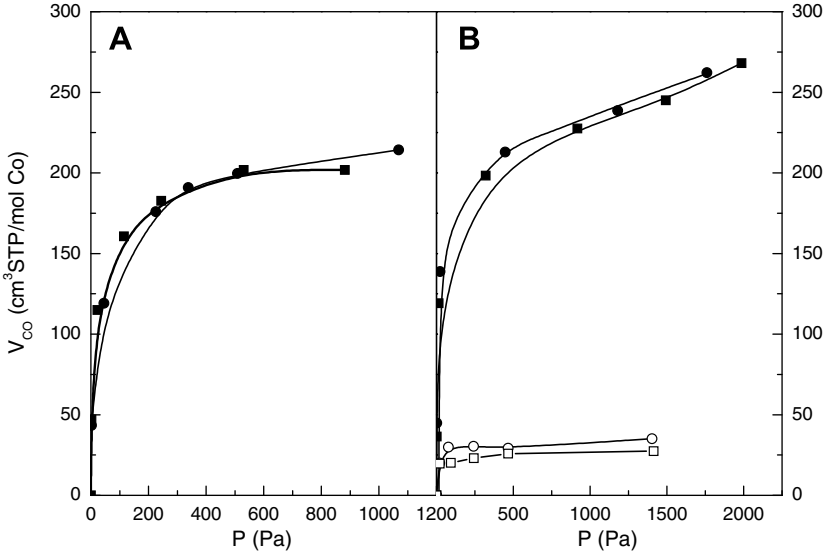

Fig. 3. CO adsorption isotherm at 298 K. A: Co–H–L, B: Co–H–Z and Co/H–Z. ●, ○: CO treated, ■, □: calcined. Closed symbol: prepared by ionic exchange, open symbol: prepared by wet impregnation method.

In order to study the effect of cobalt oxides on the CO adsorption capacity, the CO adsorption on Co-impregnated samples were measured. The behavior of these solids on their H- and Na-form followed the same trend, although the amount of the CO adsorbed resulted remarkably lower.

FTIR spectra of oxidized and CO treated samples after CO adsorption at 12,000 Pa (Fig. 4) present an intense band around 2204 cm^{-1}. This band shows a composite tail on the low frequency side in which two components are seen at about 2179 and 2163 cm^{-1}. These two bands, which also appear in the Na-MOR zeolites, are due to CO adsorbed on Na^+ located in the main channels and CO adsorbed on Na^+ located in the smaller channels, respectively [17]. It was already reported that the adsorption of CO on Co–Na-MOR yielded a strong peak at 2205 cm^{-1} with a shoulder at 2191 cm^{-1}, both arising from cobalt carbonyls [18]. Even though the shoulder is not clearly seen, the curve fitting shows the existence of this band in our spectra (Fig. 5). Analyses of the peaks were performed using Gaussian curves; R^2 was always higher than 0.998. The band at 2205 cm^{-1} was assigned to the C—O stretching vibrations of CO interacting with Co^{2+} located in the main channels (α-type Co ions), and the band at 2191 cm^{-1} to CO interacting with Co^{2+} in the smaller channels (β-type Co ions).

Table 2 shows the ratio between the integrated intensities of bands at 2191 cm^{-1} (β-type Co ions) and the band at 2205 cm^{-1} (α-type Co ions) that arises in an atmosphere of 12,000 Pa of CO. Na containing zeolites clearly show an increase of Co^{2+} located in the main channels in detriment of Co^{2+} located in the side-pockets after the CO treatment.

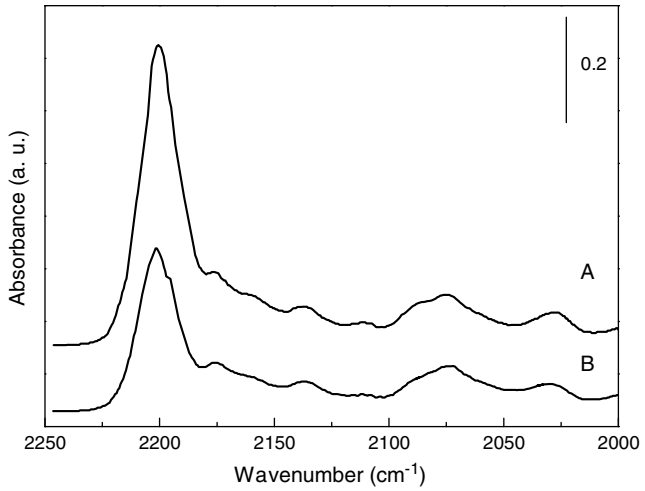

Fig. 4. FTIR spectra of CO adsorbed on: (A): calcined and (B): treated Co–Na–Z. Equilibrium pressure of 12,000 Pa.

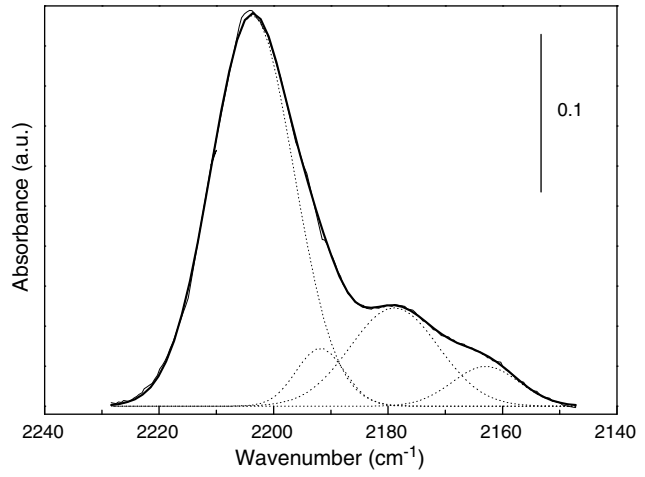

Fig. 5. Deconvolution of CO-FTIR spectra of calcined Co–Na–Z. Equilibrium pressure of 12,000 Pa.

Table 2
I_{2191}/I_{2203} ratio in calcined and CO treated ion exchanged solid in the presence of CO (12,000 Pa)

	Co–Na–L	Co–Na–Z	Co–H–L	Co–H–Z
Calcined	0.076	0.089	0.115	0.305
CO treated	0.026	≈0	0.118	0.298

On the other hand, this treatment does not affect exchanged cation distribution in acid solids. These results would confirm the hypothesis proposed by Miró and Petunchi [10]. It is interesting to notice that the β-type Co ions/α-type Co ions ratio is higher in the acid solids.

Besides the already mentioned bands, spectra of oxidized and treated samples show the presence of weak bands at 2115, 2088 and 2076 cm^{-1} which, according to Hadiivanov et al. [19], could be assigned to carbonyls of Co^{+}. The small band at 2138 cm^{-1} can be assigned to physisorbed CO [20]. Reduction of the sample in a CO atmosphere results in the creation of a fraction of Co^{+} cations that disappear in the presence of oxygen but are partly restored during evacuation. Nevertheless, Co^{+} and physisorbed CO are present in rather small amounts, Co oxides and cobalt at exchange position being the main species present in the catalysts studied in this work.

3.3. NO adsorption: FTIR study

3.3.1. NO_{ads} vibration region

NO is a strong Lewis base and, when it has a α-bonded interaction it is more firmly adsorbed on cationic sites. Besides, the presence of an unpaired electron in the molecule determines the trend of NO to adsorb as dimmers [21].

In order to obtain some information about the adsorbed NO species and their interaction with the exchanged Co sites, the IR spectra of the catalyst after the adsorption of NO are obtained. Fig. 6A and B shows IR spectra (starting from 2200 cm^{-1}) of NO adsorbed on Co–Na–L under different treatments, recorded at room temperature in flowing He. After evacuation at different temperatures, the main bands at 1940, 1897 and 1809 cm^{-1} were monitored. Bands at 1809 cm^{-1} and 1897 cm^{-1} were assigned to dinitrosyl species (Co^{2+}-$(NO)_2$) with 1809 cm^{-1} being the asymmetric stretching frequency, and 1897 cm^{-1} the symmetric stretching frequency. These two bands are associated with the adsorption of NO in α-type Co^{2+} species [22]. The signal at 1940 cm^{-1} was assigned to β-type Co^{2+} by some authors [21,23], although Ivanova et al. assigned this IR band to Co^{3+}–NO on Co-ZSM-5 catalyst [24]. The band at 2133 cm^{-1} corresponding to NO^{+} [24], observed by these authors was not present in any of our catalysts.

After evacuation at 298 K, the three bands mentioned above were present in both solids. The mononitrisyl species (1940 cm^{-1} band) seems to be more stable in the catalysts treated in flowing oxygen as it still remains at 573 K while in the CO treated solid this band almost disappears at 423 K. This fact could be related to the lower β-type Co^{2+}/α-type Co^{2+} ratio observed in the CO treated solid by CO adsorption measurements (Table 2). The cobalt oxide present in the calcined solid (Table 1 and Table 3) could also contribute to the NO adsorption [23,24].

The dinitrosyl band in the calcined sample is broader than in the CO treated sample. This could be explained by the presence of two overlapping asymmetric vibrational bands around 1815 cm^{-1} arising from two similar adsorption centers (α-type Co^{2+}) with different neighborhood. These adsorption centers are likely to be exchangeable sites IV and VI (nomenclature from [25]) located at the main channel on the mordenite structure where both sites have enough room for the dinitrosyls to form. Even though the contribution of NO adsorbed on highly dispersed cobalt oxide to these bands cannot be ruled out [26].

The dihedral angle of the dinitrosyl species can be calculated from the ratio of the integrated intensities [25]

$$I_{\mathrm{asym}}/I_{\mathrm{sym}} = \tan^2(\theta)$$

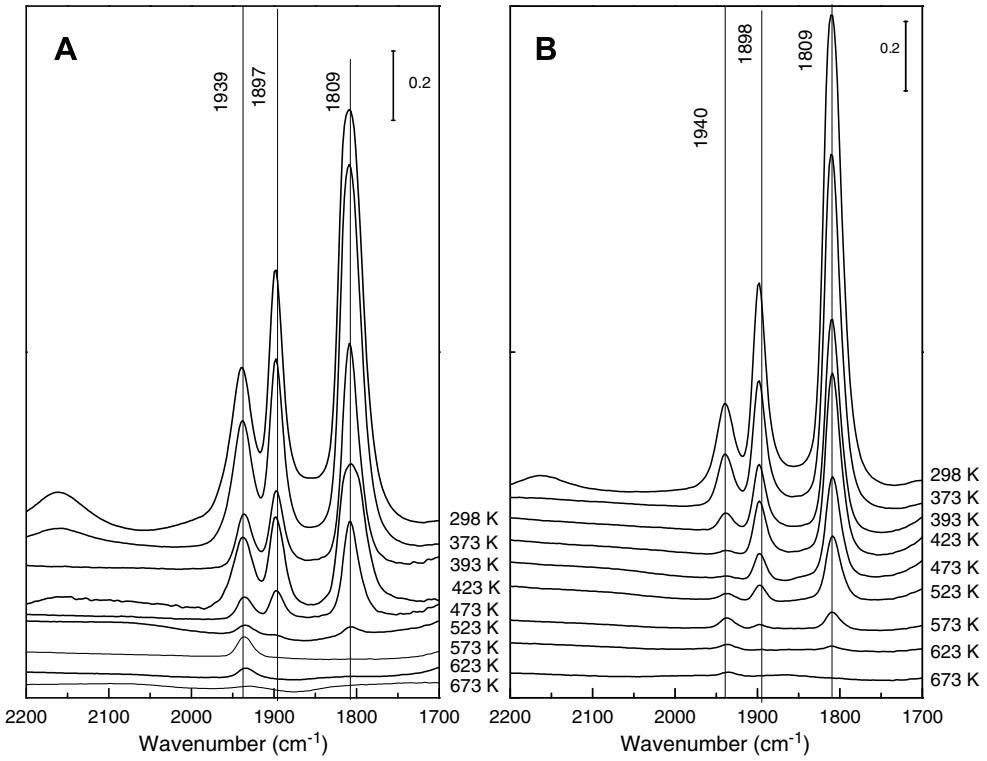

Fig. 6. IR spectra of NO adsorbed on Co–Na–L, at different temperatures recorded at room temperature. Pretreatment: (A): calcined, (B): CO treated.

where I_{asym} is the asymmetric stretching mode and I_{sym} is the symmetric stretching mode of dinitrosyl species. The relationship between I_{asym} and I_{sym} is shown in Fig. 7; a non-linear correlation is observed in the calcined sample, which would confirm that two distinctive dinitrosyl species are present, while the narrow dinitrosyl band observed in

Table 3
XPS data of the fresh and CO treated ion exchanged and impregnated solids

Sample	Treatment	Co $2p_{3/2}$ Binding energy, eV (FWHM) (area %)			Si/Al
Co–Na–L	Calcined	782.1 (3.6)	780.3 (1.3)		(5.0)[a]
		92%	8%		5.8
	$CO + O_2$	781.9 (2.9)		778.8 (1.9)	6.4
		89%		11%	
Co–Na–Z	Calcined	782.0 (3.0)	780.9 (1.7)		(6.5)[a]
		94%	6%		6.1
	$CO + O_2$	781.7 (3.2)	–	779.1 (2.0)	5.7
		78 %		22%	
Co–H–L	Calcined	782.7 (2.4)	780.4 (1.8)		(5.0)[a]
		93%	7%		6.7
	$CO + O_2$	782.6 (2.6)	–	779.5 (1.6)	6.9
		93%		7%	
Co–H–Z	Calcined	783.0 (2.2)	780.6 (2.1)		(6.5)[a]
		92%	8%		7.6
	$CO + O_2$	782.6 (2.6)	–	779.6 (2.3)	7.1
		93.5%		6.5%	
Co/Na–Z	Calcined	782.6 (3.5)	780.0 (3.6)	–	(6.5)[a]
		6%	94%		6.6
	$CO + O_2$	782.2 (3.5)	780.2 (2.8)	778.8 (3.0)	6.1
		22%	46%	32%	
Co/H–Z	Calcined	783.0 (3.2)	780.7 (2.9)		(10.0)[a]
		17%	83%		12.0
	$CO + O_2$	782.6 (3.5)	780.9 (3.1)	779.3 (2.3)	11.9
		45%	22%	33%	

[a] Bulk value.

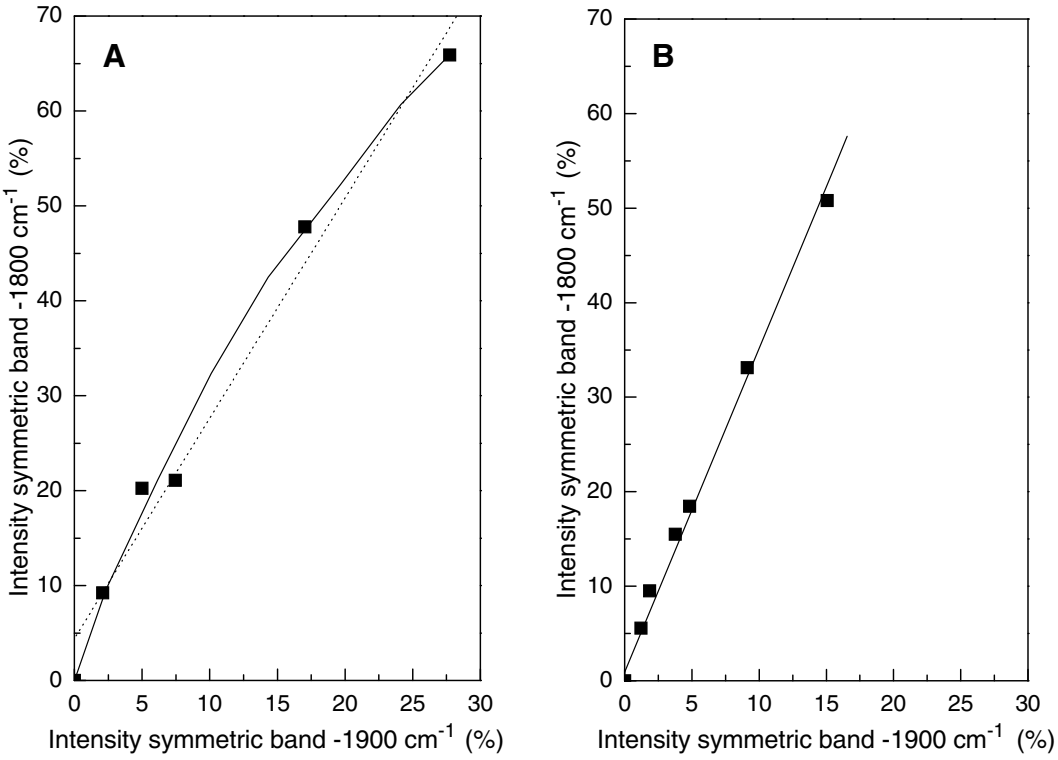

Fig. 7. Correlation of dinitrosyl symmetric and asymmetric bands. Co–Na–L. Pretreatment: (A): calcined, (B): CO treated.

the treated sample suggests the presence of one major α-cobalt species. In addition, the concentration of cobalt oxide in this solid is lower than before treatment (TPR results) and was not detected by XPS. A very similar behavior was observed in the Co–Na–Z.

In the spectra of the calcined Co–H–Z (not shown) dinitrosyl and mononitrisyl bands adsorbed on exchanged Co^{2+} and CoO_x respectively, can be observed. The mononitrosyl band remains up to 473 K while the dimmer species remain up to 523 K. After this sample was treated with CO, both mono and dinitrosyl species became more stable since bands do not disappear up to 623 K.

Fig. 8A and B report the spectra obtained during the NO desorption of calcined and CO treated Co/H–Z. In the calcined solid, bands associated with dinitrosyl and mononitrisyl species remain up to 523 K. These bands would be associated with the adsorption of NO on exchanged Co^{2+}, since 17% of the cobalt ions are at exchange positions (Table 3). The cobalt oxide could also contribute to the NO adsorption. After this sample was treated with CO, an important increase in the NO adsorption was observed, in agreement with the migration of cobalt to exchange sites.

There is no adsorption of NO as mono or dinitrosyl in the calcined Co/Na–Z impregnated samples; this could be due to the presence of Co-oxide particles blocking up the zeolite channels (Table 3). Some nitrate-like species are observed at 1410–1390 cm^{-1}, suggesting that NO is oxidized on the surface of these oxide particles, while part of the Co-oxide is reduced. This effect is favored by the presence of Na [27]. On the other hand, in the impregnated Co/Na sample after CO treatment some weak NO adsorption bands were observed in the 298–323 K range. This could be explained by the fact that in these solids part of the cobalt was reduced by the CO treatment to Co^0 and the amount of exchange cobalt was increased as found by XPS. The metallic cobalt would also prevent the formation of NO nitrate-like species [27].

3.4. Acidity measurements

The CO adsorption capacity of zeolites could be related to the number and type of available acid sites (Brønsted or Lewis). In order to learn about the acidity of calcined and CO treated solids, the species obtained from the adsorption of pyridine on the solids were monitored by FTIR. The spectrum of the Co–H–L calcined solid (Fig. 9) shows that pyridine adsorption gives rise to the appearance of bands relative to Brønsted (1540 and 1488 cm^{-1}) and Lewis sites (1488 and 1450 cm^{-1}) [28]; the CO treatment did not change the acidity of this solid. A different behavior was observed in the Na based catalyst (Co–Na–L); the FTIR spectrum of the calcined solid (Fig. 9) shows the presence of Lewis sites (1488 and 1450 cm^{-1}) only. The intensity of these bands suffers an important decrease after the CO treatment and a band at 1540 cm^{-1} would indicate the presence of Brønsted acid sites.

The amount of adsorbed Py at Lewis sites is higher in the calcined Co–Na–L catalyst, indicating that cobalt is more accessible than in the Co–H–L solid. This is in agree-

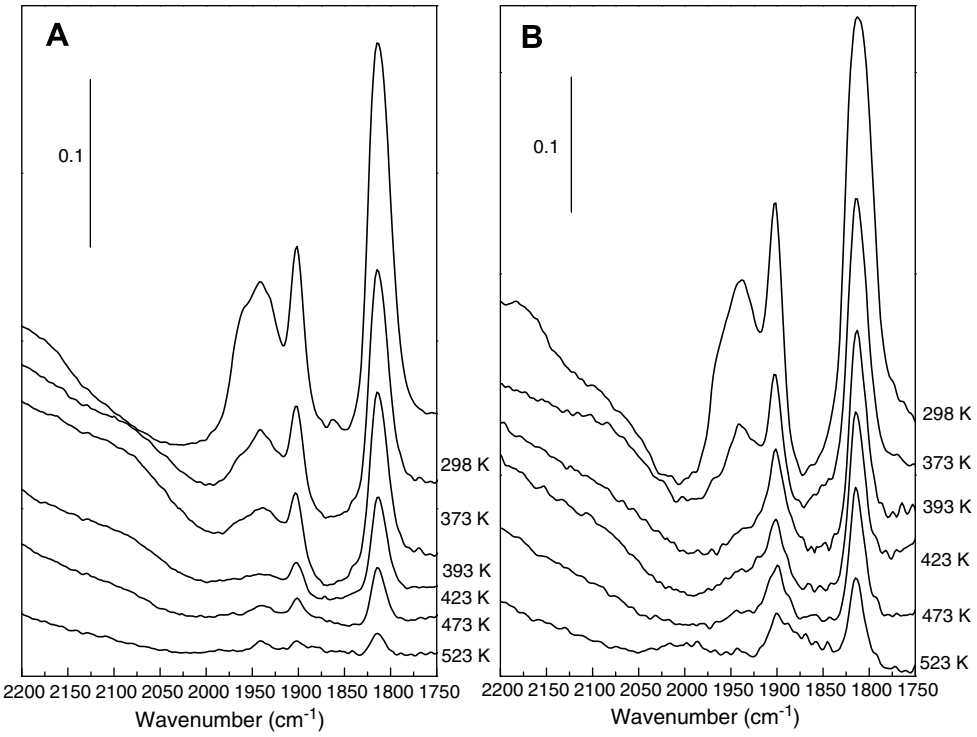

Fig. 8. IR spectra of NO adsorbed on Co–H–L at different temperatures recorded at room temperature. Pretreatment: (A): calcined, (B): CO treated.

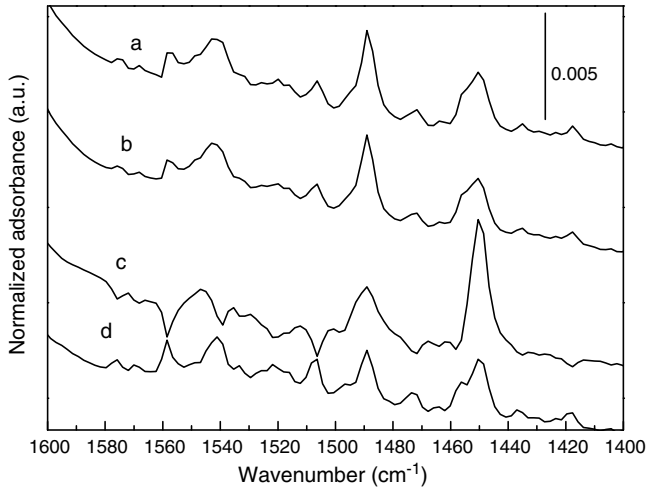

Fig. 9. IR spectra of pyridine adsorption at 673 K on: (a) calcined Co–H–L, (b) CO treated Co–H–L, (C) calcined Co–Na–L, (b) CO treated Co–Na–L.

ment with TPR results, where cobalt was reduced at lower temperature. While on the calcined and treated Co–H–L sample and on the treated Co–Na–L this band is weaker than in the calcined Co–Na–L.

3.5. XPS data

The binding energies (BE) of Co $2p_{3/2}$ core-level of the samples after different treatments are summarized in Table 3. The main peak at 782 eV in the Na calcined solids is characteristic of Co^{2+}-exchanged zeolites [29,30]. On the other hand, shoulders around 780 and 781 eV would be related to cobalt ions in cobalt oxide [31]. As the BEs for several cobalt compounds (i.e. CoO, Co_3O_4 and Co_2O_3) are very close [22], the peak around 780.5 eV cannot be assigned to a particular oxide. After treatment with CO, the Co $2p_{3/2}$ main peaks slightly shift to lower binding energies and peaks associated with cobalt oxides disappear. Besides, an additional peak around 779 eV is detected, which would correspond to metallic cobalt. These features would indicate that cobalt oxide and part of the exchanged ions reduced by CO remains as Co^0 even after the oxygen treatment. These effects would be stronger in the Co–Na–Z solid.

In the acid calcined samples, the Co $2p_{3/2}$ peaks assigned to exchange ions shift to higher energy values, ca. 783.0 and 782.7 eV. This shift with respect to the values observed in the Na catalysts would indicate a more oxidized environment in these solids [29]. There is no shift in the BE of the peaks associated with cobalt oxides with respect to the Na solids. After the CO treatments, the peaks associated with cobalt oxide disappear as in the Na solids, but there is no significant shift on the BE of Co $2p_{3/2}$ main peaks. The concentration of the new signals at 779.6 and 779.5 eV, which would correspond to metallic cobalt, is the same as the concentration of oxide in the calcined solids. In these solids, the Co oxide species was apparently the only one that remains reduced after the treatment.

Solids prepared by impregnation presented a different behavior; the CO treatment not only reduced part of the cobalt (peaks at 779.1–779.6 eV appear) but there was also an increase in the concentration of Co at exchange posi-

tions, from 6% to 22% in the Na zeolite and from 17% to 45% in the acid solid. This would indicate that in this case the same ion exchange was taking place during the high temperature treatments.

3.6. Catalytic test

The previous results did not show significant differences between the solids prepared starting from zeolysts (Z) or linde (L) mordenite. As a consequence, catalysts based on Na–Z and H–Z were chosen for the catalytic tests.

The selective catalytic reduction of NO_x with methane was used as test reaction. Fig. 10 shows the activity of solids prepared on zeolyst material by ionic exchange.

It is known that the active species for this reaction is the cobalt exchanged inside the zeolitic matrix [2–4,7,14], whereas the presence of cobalt oxides drives to the oxidation of the methane diminishing the selectivity. On the other hand, it has been demonstrated that the presence of different kinds of exchanged cobalt inside the zeolite leads to different catalyst reactivity [6]. The lower activity on the calcined Co–H–Z compared to the Co–Na–Z would be associated with the lower concentration of cobalt ions in α-positions observed in the acid solid (Table 2).

The catalytic behavior of Co–Na–Z and Co–H–Z solids after treatment B pointed out a significant drop of the active sites for NO reduction to N_2. On the other hand, the methane conversion was complete, meaning that all the hydrocarbon reacted with O_2, the changes produced by the treatment favoring the latter reaction.

In agreement with the catalysts characterization, catalytic results point to the fact that on calcined Co–Na – the main component is Co^{2+} at more exposed sites, while on treated CoNa and both (treated and calcined) CoH solids, this species migrate to hidden positions and/or remain reduced after the CO treatment.

The NO to N_2 conversion of Co-impregnated samples was lower than 10% for calcined and treated solids as a consequence of the presence of cobalt oxides that is known to produce loss of selectivity.

4. Discussion

The preparation method introduces considerable differences between cobalt species into the zeolitic matrix. During the ionic exchange method, Co^{2+} from the diluted cobalt acetate solution can migrate into the matrix channels occupying exchange positions after the calcination treatment. Samples were prepared starting from linde and zeolyst mordenites, both showing a similar behavior on TPR, XPS and CO adsorption experiments. On the other hand, the impregnation method involves the complete evaporation of the concentrated cobalt acetate solution and the precursor salt remains on the zeolitic surface and during the calcination treatment it is decomposed and the cobalt oxides are formed. Nevertheless, it is possible that during the evaporation and the treatment some cobalt is exchanged in the zeolitic matrix as was detected by TPR and XPS techniques.

The redox CO treatment applied to Co-MOR has different effects depending on the acidity of the zeolite. On H-MOR based solids the acidity was not affected by the treatment, while on the Co–Na catalysts there was an important decrease in Lewis acidity. On Na zeolites TPR results point

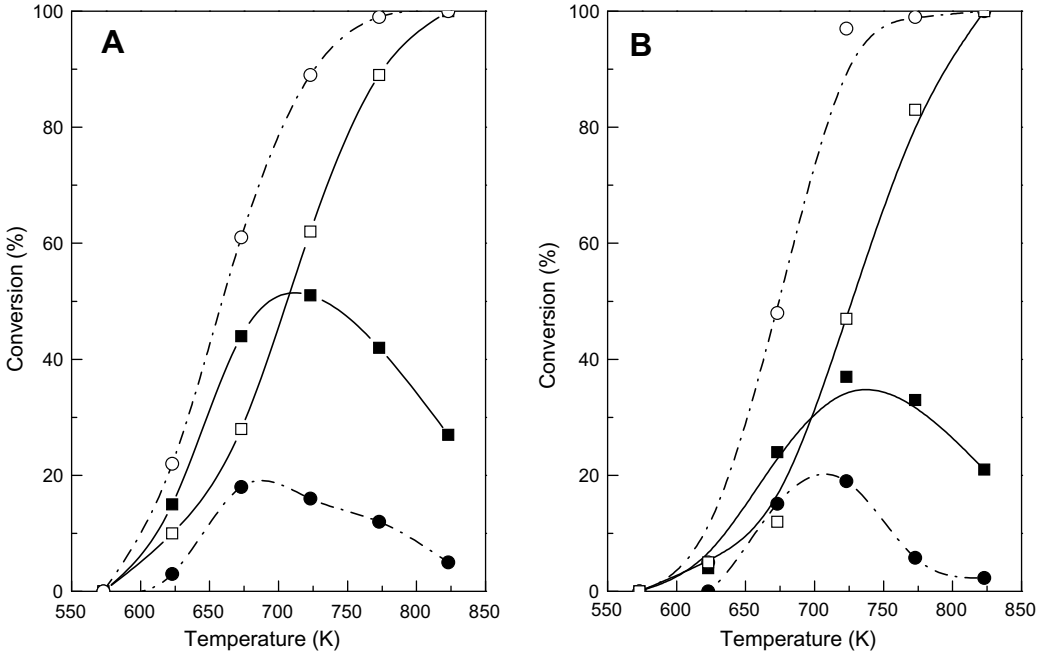

Fig. 10. Catalytic data. (A): Co–Na–Z, (B): Co–H–Z: Closed symbol: NO to N_2 conversion; open symbol: CH_4 to CO_2 conversion. Solid line: Calcined; Dot line: CO treated. Reaction conditions: see experimental.

to the decrease in the presence of cobalt oxides. These, combined with XPS results, would indicate that part of the oxides are irreversibly reduced by means of the CO redox treatment. This would also be in agreement with the acidity measurements, since the band at 1450 cm^{-1} related to pyridine molecules linked to Co^{2+} [3], diminished after the CO treatment only on Na based solids. Another important effect of this treatment would be the mobility of exchanged cobalt cations from β-type sites to the more accessible α-sites; these movements only take place in sodium solids. According to NO adsorption results, in sodium samples after treatment one of the two similar adsorption centers located at the main channel on the mordenite structure vanishes, leaving one major α-cobalt species.

Even though in the catalytic evaluations the same selectivity trend was observed after the CO treatment in all the samples, for Na solids the loss of selectivity is more important than for the acid catalysts. According to the XPS results, the cobalt oxides present in the calcined samples are eliminated by the treatment. Therefore, the decrease in selectivity cannot be related to these species. The reduction of an important part of the cobalt in active sites to metallic Co shown by XPS would be the cause for the loss of selectivity of the treated Co–Na–Z solid, even when the exchanged Co^{2+} ions are in more accessible sites (Table 2). Besides, the activity of the two α-type exchangeable sites IV and VI, located at the main channel on the mordenite, would be different since the presence of one major α-cobalt species (NO adsorption results) leads to a lower selectivity.

According to the XPS results, in the treated acid solids there was only reduction of the superficial cobalt oxides without loss of the active sites. In this case, the position of Co ions inside the zeolite structure would play a major role in the selectivity. The most populated β-type Co ions, which do not migrate under treatment (Table 2), could be reduced by the CO at high temperature, not only diminishing the active sites concentration but also blocking the channels and preventing the access of the reactants. This would also agree with the increase in the reduction temperature observed by TPR. The surface sensitivity of the XPS technique would not allow measuring these changes in the inside of the zeolitic crystals. On the other hand, the strong adsorption of NO detected by FTIR could be in part responsible for the loss of selectivity [23].

5. Conclusions

The treatment of Co-exchanged mordenite catalysts with redox cycles with CO/O_2 leads to different results depending on the counter cation of the zeolite matrix.

- During the CO treatment some stable nanoparticles of metallic cobalt are formed and these remain after the O_2 calcination (treatment B) (XPS results).
- In Co-Na, the treatment increases the CO adsorption capacity probably due to the reduction of cobalt oxides (XPS and TPR results) and the migration of exchanged Co^{2+} ions from β-type sites to α-type sites (FTIR results) and the decrease of one of the two α-type exchangeable sites (NO adsorption results). These two processes would lead to a lower concentration of Lewis acid sites. All these changes cause a lower activity of the Na-MOR solids in the selective catalytic reduction of NO_x with methane.
- In Co–H, cobalt exchange ions are mainly in β-type sites. Experimental evidence of the redox treatment in these solids only indicates higher temperature reduction (TPR), reduction of superficial oxides (XPS), low amount of exposed Lewis sites for pyridine adsorption and a stronger adsorption of NO. No change in the CO adsorption was observed and no migration of exchanged ions inside the zeolitic frameworks was detected by FTIR. The lower selectivity in the catalytic reduction of NO_x with methane after treatment could be due to the stronger adsorption of NO. Besides, the reduction of β-type Co^{2+} to metallic cobalt could decrease the active sites concentration and also block the channels and prevent the access of the reactants. Cobalt oxide species could be exchanged during redox cycles with CO/O_2.

Acknowledgments

The authors wish to acknowledge the financial support received from UNL, CONICET and ANPCyT. They are also grateful to the Japan International Cooperation Agency (JICA) for the donation of the major instruments used in this study. Thanks are given to Elsa Grimaldi for the English language editing, to Horacio Cabral for his help with the pyridine experiments, and to Leticia Gómez and Cecilia Pérez for their technical assistance. S. Irusta acknowledges support from the Spanish "Ramón y Cajal" program.

References

[1] Y.J. Li, J.N. Armor, Appl. Catal B: Env. 2 (1993) 239–256.
[2] Y.J. Li, J.N. Armor, J. Catal. 150 (1994) 376–387.
[3] L. Gutierrez, M.A. Ulla, E.A. Lombardo, A. Kovács, F. Lonyi, J. Valyon, Appl. Catal. A 292 (2005) 154–161.
[4] J. Dědeček, B. Wichterlova, J. Phys. Chem. B. 103 (1999) 1462–1471.
[5] J.N. Armor, Catal. Today 26 (1995) 147–158.
[6] D. Kaucký, A. Vondrová, J. Dědeček, B. Wichterlova, J. Catal. 194 (2000) 318–329.
[7] C. Resini, T. Montanari, L. Nappi, G. Bagnasco, M. Turco, G. Busca, F. Bregani, M. Notaro, G. Rocchini, J. Catal. 214 (2003) 179–190.
[8] A. Martínez-Hernández, G.A. Fuentes, Appl. Catal. B 57 (2005) 167–174.
[9] M.A. Ulla, L. Gutierrez, E.A. Lombardo, F. Lónyi, J. Valyon, Appl. Catal. A 277 (2004) 227–237.
[10] E. Miró, J. Petunchi, J. Chem. Soc. Faraday Trans. 88 (8) (1992) 1219–1223.
[11] G. Fierro, M.A. Eberhardt, M. Houalla, D. Hercules, W.K. Hall, J. Phys. Chem. 100 (1996) 8468.
[12] Z. Sobalík, J. Dědeček, D. Kaucký, B. Wichterlová, L. Drozdová, R. Prins, J. Catal. 194 (2000) 330–342.

[13] M.D. Sefcik, J. Schaefer, E.O. Stejkal, in: J. Katzer (Ed.), Molecular Sieve II, ACS Symp. Ser, American Chemical Society, Washington, 1977, pp. 334–342.
[14] L. Gutierrez, A. Boix, J.O. Petunchi, J. Catal. 179 (1998) 179–191.
[15] D. Kaucký, J. Dědeček, B. Wichterlová, Microp. Mesop. Mater. 31 (1999) 75.
[16] F. Bustamante, F. Córdoba, M. Yates, C.M. de Correa, Appl. Catal. A 234 (2002) 127–136.
[17] S. Bordiga, C. Lamberti, F. Geobaldo, A. Zecchina, Langmuir 11 (1995) 527.
[18] M. Campa, I. Luisette, D. Pietrogiacomi, V. Indovina, Appl. Catal. B 46 (2003) 511–522.
[19] K. Hadjiivanov, B. Tsyntsarski, Tz. Venkov, M. Daturi, J. Saussey, J. Lavalley, Phys. Chem. Chem. Phys. 5 (1993) 243–245.
[20] T. Montanari, O. Marie, M. Daturi, G. Busca, Appl. Catal. B 71 (2007) 216.
[21] K. Hadjiivanov, H. Knödzinger, Chem. Phys. Lett. 303 (1999) 513–520.
[22] L.B. Gutierrez, A.V. Boix, E.A. Lombardo, J.L.G. Fierro, J. Catal. 199 (2001) 60–72. Q1
[23] L. Gutierrez, E.E. Miró, M.A. Ulla, Appl. Catal. A 321 (2007) 7–16.
[24] E. Ivanova, K. Hadjiivanov, D. Klissurski, M. Bevilacqua, T. Armaroli, G. Busca, Microp. Mesop. Mater. 46 (2001) 299–309.
[25] W. Mortier, J. Phys. Chem. 81 (1977) 1334.
[26] N.-Y. Topsøe, H. Topsøe, J. Catal. 75 (1982) 354–374.
[27] C. Henriquez, O. Marie, F. Thibault-Starzyk, J.-C. Lavalley, Microp. Mesop. Mater. 50 (2005) 167–171.
[28] O. Busch, W. Brijoux, S. Thomson, F. Schüth, J. Catal. 222 (2004) 174–179.
[29] J. Stencel, V. Rao, J. Diehl, K. Rhee, A. Dhere, J. De Angelis, J. Catal. 84 (1983) 109–116.
[30] S. Verberckmoes, B. Weckhuysen, R. Schoonheydt, Microp. Mesop. Mater. 22 (1998) 165–178.
[31] A. Boix, E. Miró, E. Lombardo, R. Mariscal, J.L.G. Fierro, Appl. Catal. A 276 (2004) 197–205.